

## Reconstructing random media

C. L. Y. Yeong and S. Torquato

*Department of Civil Engineering and Operations Research and Princeton Materials Institute,  
Princeton University, Princeton, New Jersey 08540*

(Received 6 August 1997)

We formulate a procedure to reconstruct the structure of general random heterogeneous media from limited morphological information by extending the methodology of Rintoul and Torquato [J. Colloid Interface Sci. **186**, 467 (1997)] developed for dispersions. The procedure has the advantages that it is simple to implement and generally applicable to multidimensional, multiphase, and anisotropic structures. Furthermore, an extremely useful feature is that it can incorporate any type and number of correlation functions in order to provide as much morphological information as is necessary for accurate reconstruction. We consider a variety of one- and two-dimensional reconstructions, including periodic and random arrays of rods, various distribution of disks, Debye random media, and a Fontainebleau sandstone sample. We also use our algorithm to construct heterogeneous media from specified hypothetical correlation functions, including an exponentially damped, oscillating function as well as physically unrealizable ones. [S1063-651X(98)01701-2]

PACS number(s): 44.30.+v

### I. INTRODUCTION

The reconstruction of random heterogeneous media, such as porous and composite media, from a knowledge of limited morphological information (correlation functions) is an intriguing inverse problem. An effective reconstruction procedure enables one to generate accurate structures at will, and subsequent analysis can be performed on the image to obtain desired macroscopic properties (e.g. transport, electromagnetic, and mechanical properties) of the media. This provides a nondestructive means of estimating the macroscopic properties: a problem of important technological relevance. However, it is clear that even if the correlation functions of the reference and reconstructed systems are in good agreement, this does not ensure that the structures of the two systems will match very well. This interesting question of nonuniqueness can also be probed using reconstruction methodologies. Another useful application is the reconstruction of a three-dimensional (3D) structure using information obtained from a two-dimensional (2D) micrograph or image. Such reconstructions are of great value in a wide variety of fields, including petroleum engineering, biology, and medicine, because in many cases only 2D images are available for analysis. A further intriguing inverse problem that has been suggested [1] is the construction of heterogeneous media based on the specification of a model or hypothetical statistical correlation function. This question involves understanding the general mathematical properties of realizable correlation functions. Finally, we note that reconstruction procedures can shed light on the nature of the information contained in the statistical correlation functions that are implemented. This potentially can aid one in identifying the appropriate correlation functions that can effectively characterize a class of structures.

There are a number of approaches that have been taken to reconstruct random media [2–15]. An extensively examined reconstruction method is based on successively passing a normalized uncorrelated random Gaussian field through a linear and then a nonlinear filter to yield the discrete values

representing the phases of the structure. One approach was originated by Joshi [2] and extended by Quiblier [3] from 2D to 3D reconstructions. Adler *et al.* [4] refined the technique to accommodate periodic boundary conditions. The linear filter in this method convolutes linearly the independent Gaussian field, giving another field that is still Gaussian distributed but correlated. The nonlinear filter then performs a threshold cut to the field to generate the final reconstructed structure. Through this nonlinear filter, the statistical properties of the transformed field are related to that of the reference structure, and the problem leads to solving a nonlinear system of equations (e.g., by optimization methods) to determine the coefficients of the linear filters. This procedure has been further modified [5–7] as well.

Another approach, which is based also on filtering, was originally devised by Cahn [8] and was analyzed in detail and applied by a number of investigators [9–14]. This approach differs from the aforementioned one in that the linear filter has a different functional form, and it includes double-level (apart from single-level) thresholding the corresponding correlated Gaussian random fields. The method is found to reconstruct well many classes of nonparticulate composite materials, such as Vycor glass and membrane systems. However, the class of random media for which it works well is limited by virtue of the use of Gaussian random field. For example, as reported by Levitz [14], the process does not reconstruct particulate systems (such as soils) satisfactorily. He noted that more morphological information beyond that contained in the standard two-point probability function (described in Sec. II B) is required to reconstruct these structures.

The aforementioned filtering methods have been formulated for the reconstruction of two-phase isotropic media using *standard* one-point (volume fraction) and the two-point correlation function information. These approaches are limited in that they are difficult to extend to and incorporate other correlation functions for two-phase isotropic media and are practically impossible to extend to general multiphase and anisotropic media.

The method we propose to reconstruct random media is a variation of the simulated annealing method introduced by Rintoul and Torquato [15] who originally used the method to reconstruct dispersions of particles. In the present work, we extend the method to reconstruct random media of arbitrary topology by considering digitized representations of the systems. The procedure involves finding a state of minimum ‘‘energy’’ among a set of many local minima by interchanging the phase of pixels in the digitized system. The energy is defined in terms of a sum of the squared difference of the reference and simulated correlation functions. The reconstruction procedure that we propose has a number of useful features; it is (i) simple to implement, (ii) generally applicable to multidimensional, multiphase, and anisotropic structures, (iii) extendable to include any type and number of correlation functions as microstructural information, and (iv) can be used to construct heretofore unknown structures from specified correlation functions (even physically unrealizable ones).

The outline of the rest of the paper is as follows: In Sec. II, we formulate the reconstruction procedure for digitized media. In particular, we will utilize the information contained in the two-point probability function  $S_2$ , the lineal-path function  $L$ , and the combination of these two correlation functions ( $S_2$  and  $L$ ), although other functions could also have been used. In Sec. III, we apply the procedure to a variety of one-dimensional (1D) models, including a case where we specify an unphysical correlation function. In Sec. IV, we employ the reconstruction technique to a number of different 2D models. In Sec. V, we make concluding remarks.

## II. FORMULATION OF THE RECONSTRUCTION PROCEDURE

### A. General procedure

The reconstruction methodology employed here follows closely the one introduced by Rintoul and Torquato [15] but is modified for use in digitized media. Thus, we are not only able to carry out reconstructions for dispersion of particles, but for anisotropic multiphase systems of arbitrary topology. For simplicity, we will begin by outlining the reconstruction procedure by considering only a single two-point correlation function for statistically isotropic two-phase media. This is followed by a description of a more general procedure incorporating a set of different  $n$ -point correlation functions for anisotropic multiphase systems.

Consider reconstructing a two-phase isotropic medium where the ‘‘reference’’ two-point correlation function  $f_0(r)$  of phase  $j$  (equals to 1 or 2 in this case) is provided. Here, the quantity  $r$  is the distance between two points in the system. Let  $f_s(r)$  be the same correlation function of the reconstructed digitized system, with periodic boundary conditions, at some time step. It is this system that we shall attempt to evolve towards  $f_0(r)$  from an initial guess of the system configuration.

Once  $f_s(r)$  at a particular time step is evaluated, a variable  $E$  that plays the role of the energy in the simulated annealing can be calculated as

$$E = \sum_i [f_s(r_i) - f_0(r_i)]^2. \quad (1)$$

To evolve the digitized system towards  $f_0(r)$  (or in other words, minimizing  $E$ ), we interchange the states of two arbitrarily selected pixels of different phases. This phase interchange procedure has the nice property of automatically preserving the volume fraction of both phases during the reconstruction process. After the interchange is performed, we can calculate the energy  $E'$  of the resulting state and the energy difference  $\Delta E = E' - E$  between two successive states of the system. This phase interchange is then accepted with probability  $p(\Delta E)$  via the Metropolis method as

$$p(\Delta E) = \begin{cases} 1, & \Delta E \leq 0 \\ \exp(-\Delta E/T), & \Delta E > 0, \end{cases} \quad (2)$$

where  $T$  is the ‘‘temperature.’’ This method causes  $f_s(r)$  to converge gradually to  $f_0(r)$ . The cooling schedule, which governs the value and the rate of change of  $T$ , is chosen to allow the system to evolve to the desired state as quickly as possible, without getting trapped in any local energy minima. We adopt the suggestion that the starting  $T$  should have a value such that the initial acceptance rate is 0.5 [16]. The algorithm terminates when the energy  $E$  [given by Eq. (1)] is less than some small tolerance value or when the number of consecutive unsuccessful phase interchanges is greater than a large number ( $\sim 20\,000$ ). At the ground state, the energy  $E$  can be viewed as a *least-squares* error.

The reconstruction procedure can be generalized to apply to an anisotropic multiphase system. This is done by using a reference two-point correlation function as  $f_0^{(j)}(\mathbf{r})$ , where  $\mathbf{r}$  is the position vector and  $j$  indicates the phase number of up to  $p$  for a  $p$ -phase system. One can even extend the process to employ  $m$  different  $n$ -point correlation functions  $f_0^{(j,k)}(\mathbf{r}^n)$  where  $k = 1, \dots, m$ , and each function depends upon  $n$  different positions  $\mathbf{r}^n = \mathbf{r}_1, \dots, \mathbf{r}_n$  (see Ref. [15]). The accompanying  $f_s$ 's are defined in a similar way.

The energy can now be defined as

$$E = \sum_i \sum_j \sum_k \alpha_{j,k} [f_s^{(j,k)}(\mathbf{r}^n) - f_0^{(j,k)}(\mathbf{r}^n)]^2, \quad (3)$$

where the sum on  $i$  is multidimensional over all configurations of  $\mathbf{r}^n$ . The quantity  $\alpha_{j,k}$  in the expression is an arbitrary weight that assigns the relative importance of each individual correlation function contributing to the total energy. This parameter can even depend on the stage of reconstruction, so that suitable correlation functions can be used at the initial stage to hasten the convergence to a crude structure, and then other correlation functions can be used at the end to refine the reconstructed image.

There are a variety of correlation functions that can be used in the reconstruction procedure, including the two-point probability function [17], lineal-path function [18], two-point cluster function [19], chord-length distribution function [20], and pore-size distribution function [21,22], to name just a few. There exist more complicated correlation functions and we refer the reader to Ref. [23] for a thorough review. To

illustrate the reconstruction procedure, we will apply the technique to both 1D and 2D two-phase isotropic systems using the *two-point probability function*  $S_2(r)$  and the *lineal-path function*  $L(r)$ . These two correlation functions contain substantial structural information and yet are simple enough to be implemented.

### B. Two-point probability function reconstruction

The autocorrelation function of a statistically inhomogeneous system is defined as

$$S_2^{(j)}(\mathbf{r}_1, \mathbf{r}_2) = \langle I^{(j)}(\mathbf{r}_1) I^{(j)}(\mathbf{r}_2) \rangle, \quad (4)$$

where  $\mathbf{r}_1$  and  $\mathbf{r}_2$  are two arbitrary points in the system, angular brackets denote an ensemble average, and the characteristic function  $I^{(j)}(\mathbf{r})$  is defined as

$$I^{(j)}(\mathbf{r}) = \begin{cases} 1, & \text{when } \mathbf{r} \text{ is in phase } j \\ 0, & \text{otherwise.} \end{cases} \quad (5)$$

The quantity  $S_2^{(j)}(\mathbf{r}_1, \mathbf{r}_2)$  can be interpreted as the probability of finding two points at positions  $\mathbf{r}_1$  and  $\mathbf{r}_2$  both in phase  $j$ . Thus, we will refer to it as the *two-point probability function*.

For statistically isotropic media,  $S_2^{(j)}(\mathbf{r}_1, \mathbf{r}_2)$  depends only on the distance  $r = |\mathbf{r}_1 - \mathbf{r}_2|$  between two points, and therefore can be expressed simply as  $S_2^{(j)}(r)$ . For all isotropic media without long-range order,

$$S_2^{(j)}(0) = \phi_j \quad \text{and} \quad \lim_{r \rightarrow \infty} S_2^{(j)}(r) = \phi_j^2, \quad (6)$$

where  $\phi_j$  is the volume fraction of phase  $j$ . For porous solids, Debye *et al.* [24,25] developed a relationship between  $S_2(r)$  of the material phase and the scattering intensity obtained in a small-angle radiation scattering experiment. It should be emphasized that the two-point probability function cannot distinguish between phase 1 and phase 2 materials in a two-phase system since  $S_2^{(1)}(r) - \phi_1^2 = S_2^{(2)}(r) - \phi_2^2$ . Hereafter, unless otherwise indicated, we will drop the superscript of  $S_2^{(j)}(r)$  and simply refer to  $S_2(r)$  as the two-point probability function of the phase that we are interested in reconstructing.

The specific surface  $s$  of a two-phase medium is defined as the area of the two-phase interface per unit total volume of the medium. Thus, it has the dimensions of inverse length and is an important characteristic length scale of the medium. Debye, Anderson, and Brumberger [25] showed that the slope of the two-point probability function of either phase at  $r=0$  is equal to  $-s/4$  in three dimensions. For the first three space dimensions, it is easy to show that

$$\frac{d}{dr} S_2(r) \Big|_{r=0} = \begin{cases} -s/2, & D=1 \\ -s/\pi, & D=2 \\ -s/4, & D=3, \end{cases} \quad (7)$$

where  $D$  is the space dimension.

In a *digitized* medium, although the slope in the 1D case is the same as that of a continuum medium, it is not so in 2D and 3D. The derivation is straightforward when one considers the discrete number of interfacial faces the digitized

structure has when it is constrained by  $S_2(r)$  at  $r=0$  and 1 pixel. It is simple to show that for a  $D$ -dimensional digitized medium, one has

$$\frac{d}{dr} S_2(r) \Big|_{r=0} = -s/(2D). \quad (8)$$

The discrete nature of the digitized system means that the distance  $r$  can be conveniently measured in terms of pixels and acquires integral values, with the end points of  $r$  located at the pixel centers. Also, it can be shown that when sampled along the direction of rows (or columns) of pixels,  $S_2(r)$  is a linear function between adjacent pixels:

$$S_2(r) = (1-f) S_2(i) + f S_2(i+1), \quad \text{for } i \leq r < i+1, \quad (9)$$

where  $i$  is an integer, and  $f = r \bmod 1$ . Because of this linear property, the evaluation of  $S_2(r)$  at integral values of  $r$  is sufficient to characterize the structure, and determining it for noninteger values of  $r$  is not necessary. Consequently,  $S_2^{(j)}(r)$  can be evaluated simply by successively translating a line of  $r (=i)$  pixels in length at a distance of one pixel at a time and spanning the whole image, counting the number of successes of the two end points falling in phase  $j$ , and finally dividing the number of successes by the total number of trials (which is also the system size for a periodic medium). In 1D cases, this sampling is of course performed along the single row of pixels. In 2D, we assume isotropy of the evolving system (which is not unreasonable due to the random nature of the annealing process) and the sampling is therefore performed only along two orthogonal directions: the rows and columns of pixels. It is observed that this sampling procedure can be more accurate and produces a smoother  $S_2$  profile than that by random sampling (throwing random points into the system), because the former exhaustively incorporates information from every pixel in the entire system. Of course, at additional computational cost, one could sample  $S_2$  in more directions than two orthogonal directions only.

To begin the reconstruction process, a random checkerboard with volume fraction  $\phi_j$  of the reference system is used as the initial structure, i.e., each pixel has a probability of  $\phi_j$  as phase  $j$  material. Practically, to avoid finite-size effects, the random checkerboard is constructed by randomly choosing the correct number of pixels in the system and assigning phase  $j$  to them.  $S_2(r)$  is then evaluated by the aforementioned sampling procedure over a range of  $r$ , which we will refer to as the ‘‘sampling region.’’ The structure is then altered by a phase interchange of two different pixels within the system. The resultant  $S_2$  profile of this intermediate system is calculated and accepted with probability given by Eq. (2). This annealing procedure is carried out successively until the evolving system’s  $S_2$  matches the reference  $S_2$  within a tolerance limit.

The annealing process can be made remarkably efficient by noticing that once the  $S_2$  profile of the initial structure has been determined by the sampling procedure described, there is no need to fully sample the intermediate structures all over again by the same sampling method to calculate their  $S_2$ . In fact, a change in  $S_2$  from the previous structure is only due to

the change of the success rate (occurrence of the two end points fall in phase  $j$ ) along the row and column that cross each altered pixel. This change in  $S_2$  can simply be evaluated by invoking the sampling technique *only* along those rows and columns crossing the altered pixels. Therefore, to evaluate the  $S_2$  profile of a succeeding structure,  $S_2$  of the preceding structure can be stored beforehand, and that of the subsequent structure can be updated efficiently by correspondingly adjusting the stored  $S_2$  using the calculated change.

The algorithm is made even more efficient if the size of the sampling region can be reduced. A useful fact is that  $S_2$  is an even function in a periodic medium and therefore the sampling region takes up at most half of the entire system size. However, the sampling region can be even smaller. We have found that compared to using a larger sampling region, the algorithm gives comparable results when the sampling region only encompasses a distance of at least one unit repeatable cell of the reference structure, or several pixels ( $< 10$  in a 1000 pixels system) after the long-range value of  $S_2$  has been reached, whichever is smaller.

### C. Lineal-path function reconstruction

Another important morphological descriptor of the structure of random media is the lineal-path function  $L^{(j)}(\mathbf{r}_1, \mathbf{r}_2)$ , which is defined as the probability of finding a line segment spanning from  $\mathbf{r}_1$  to  $\mathbf{r}_2$  that lies entirely in phase  $j$  [18]. This function contains some connectedness information, at least along a lineal path, and hence contains certain long-range information about the system. In an isotropic medium, the lineal-path function depends only on the distance  $r$  between the two points and can be expressed simply as  $L^{(j)}(r)$ . Clearly, for all media having a volume fraction of  $\phi_j$ ,

$$L^{(j)}(0) = S_2^{(j)}(0) = \phi_j. \quad (10)$$

Unlike  $S_2$ , a lineal-path function can distinguish between different phases of a medium, in the sense that the lineal-path function for a particular phase is not uniquely determined by simply knowing that of the complementary phase(s). Therefore, for efficient reconstruction using lineal-path functions, it is important to identify which phase in the medium is the target phase to be reconstructed. Hereafter, unless otherwise indicated, we will drop the superscript of  $L^{(j)}(r)$  and simply refer to  $L(r)$  as the lineal-path function of the phase of interest.

To evaluate  $L(r)$  in a digitized system, it is again sufficient to let  $r$  take integer values; sampling is again performed only along orthogonal directions.  $L^{(j)}(i)$  is defined to be the probability of finding a line segment of length  $(i, i+1]$  that falls in phase  $j$ . To illustrate how to evaluate  $L^{(j)}(i)$  efficiently, we first consider a simple case where only a single phase  $j$  chord of length  $\ell$  is present in a one-dimensional system. Clearly,

$$L^{(j)}(i) = \begin{cases} (\ell - i)/N, & \text{when } 0 \leq i \leq \ell \\ 0, & \text{otherwise,} \end{cases} \quad (11)$$

where  $N$  is the system size in pixels. For a system that has more chords or for a system of a higher dimension, the same



FIG. 1. Initial configuration: one-dimensional random checkerboard. System is 1000 pixels in length and volume fraction  $\phi_2 = 0.5$ .

principle applies to each of the chords such that the lineal-path function of the entire system is the sum of that due to the individual chords. In this respect, the sampling procedure to evaluate  $L$  reduces merely to a problem of identifying the lengths of the chords of the corresponding phase in the system. Provided the system is isotropic, this method of determining  $L$  is considerably more efficient than by throwing random lines into the system.

Again, as in the case of  $S_2$ , it is not necessary to fully sample all of the intermediate structures to determine their lineal-path functions during the annealing procedure. One only needs to keep track of the length of the chords being destroyed and created due to the phase interchange of pixels so that  $L$  can be efficiently updated according to these changes.

The sampling region should be chosen to encompass the range before the lineal-path function becomes negligibly small. Unfortunately, unlike  $S_2$ ,  $L$  is not an even function. The sampling region could therefore be large, and may extend beyond half of the system size, depending on the characteristic cluster size in the medium.

### D. Hybrid reconstruction

Different correlation functions contain distinctive morphological information; generally, a single lower-order function cannot fully characterize a structure. The lineal-path function  $L$  contains lineal “clustering” or “connectedness” information that is absent in the two-point probability function  $S_2$ . However, it does not contain morphological information for length scales larger than the maximum cluster size in the system. As an example,  $L$  does not differentiate between a structure of identical hard disks in a thermal equilibrium arrangement and that of random sequential addition (RSA) arrangement, i.e.,  $L(r)$  for the particle-phase is the same for both structures, since  $L(r)$  only contains correlation information within a cluster. On the other hand,  $S_2$  provides short-range information about different clusters. To overcome the weaknesses of individual correlation functions and to exploit the useful information contained in each correlation function, one can accommodate an arbitrary number of different correlation functions in the reconstruction process. The practical limitation on the number of different functions that can be used will be the computational expense that one can afford. In this paper, we will illustrate the use of multiple correlation functions by incorporating both  $S_2$  and  $L$  in the reconstruction process. We put equal weight on the importance of the functions such that  $\alpha^{(j,k)} = 1$  for all  $k$  in Eq. (3).

## III. APPLICATION TO ONE-DIMENSIONAL MEDIA

To begin with, we provide a few examples of 1D reconstructions to gain some insight about the process. In each case, the initial structure is a 1D random checkerboard with a

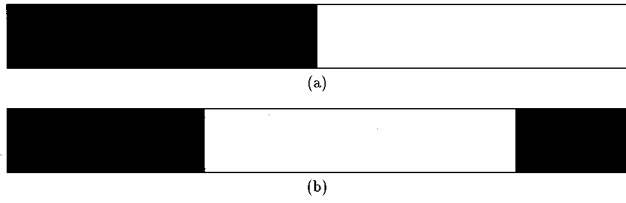


FIG. 2. (a) Reference system: unit cell of periodic rods. System size = 1000 pixels, rod length = 500 pixels, and volume fraction  $\phi_2=0.5$ . (b)  $S_2$  reconstruction of periodic rods system.

system size of 1000 pixels, and has the same volume fraction as the reference system. An example of a structure at 50% volume fraction is shown in Fig. 1. In the following, unless otherwise stated, phase 2 is the target phase of the reconstruction, and the correlation functions of phase 2 are used. In all of the images shown, this phase is represented by black pixels.

### A. Periodic rods

Consider a digitized system of periodic rods (phase 2)  $d$  pixels in length whose centers are separated by  $d$  pixels. The two-point probability function is a periodic triangular function with a period of  $2d$ :

$$S_2(r) = \begin{cases} (1-r/d)/2, & \text{when } 0 \leq r < d \\ -(1-r/d)/2, & \text{when } d \leq r < 2d, \end{cases} \quad (12)$$

$$S_2(r+2d) = S_2(r),$$

and the lineal-path function is given by

$$L(r) = \begin{cases} (1-r/d)/2, & \text{when } 0 \leq r < d \\ 0, & \text{otherwise.} \end{cases} \quad (13)$$

To show the capability of the reconstruction procedure, we will illustrate the most difficult situation where a single rod spans half of the system size ( $d=500$  pixels). To reconstruct this reference system [shown in Fig. 2(a)], the procedure needs to cluster 500 phase 2 pixels into a single connected row, which is very different from the initial structure (see Fig. 1).

The reconstructed system obtained by using  $S_2$  as the correlation function is shown in Fig. 2(b). The reconstructed system appears to be dislocated; however, due to periodic boundary conditions, a shift of the system matches exactly the reference system. The reconstruction indeed clusters the phase-2 pixels together in the necessary fashion. The reconstruction procedure using  $L$  as the correlation function (not shown) also yielded a perfect result in this case.

### B. Equilibrium hard rods

The previous example deals with the special case of 1D deterministic structures that are uniquely determined by those lower-order correlation functions. For random structures, lower-order correlation functions generally do not contain complete information and therefore cannot be expected to yield perfect reconstructions. Of course, the judicious utilization of combinations of lower-order correlation functions

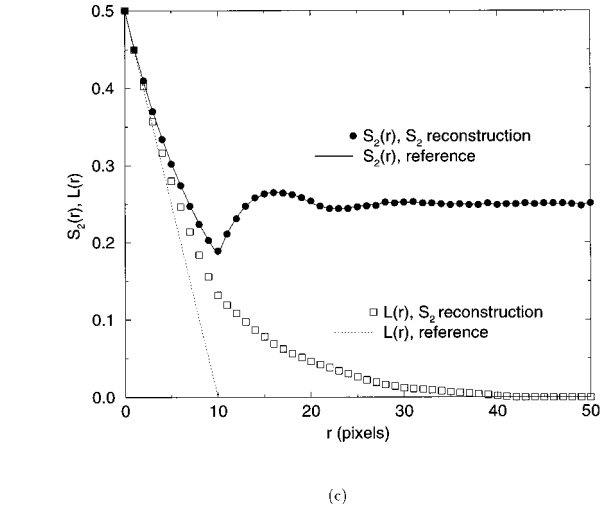
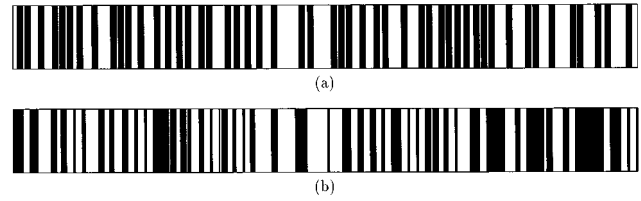


FIG. 3. (a) Reference system: a realization of equilibrium hard rods. System size = 1000 pixels, rod length = 10 pixels, and volume fraction  $\phi_2=0.5$ . (b)  $S_2$  reconstruction of equilibrium hard rods system. (c)  $S_2$  for the reference and reconstructed systems. Also shown is the lineal-path function  $L$  for both systems.

can produce more accurate reconstructions than any single function alone. This idea will be implemented as described below.

One of the random systems we investigate consists of an equilibrium arrangement of hard rods having a uniform length of  $d$  pixels. The two-point probability function  $S_2$  can be expressed analytically [26]. In a simplified form, the expression is given as [27]

$$S_2(r) = (1 - \phi_2) \sum_{k=0}^j \frac{\exp(-[r/d-k]/a) \left(\frac{r/d-k}{a}\right)^k}{k!} + 1 - 2\phi_2, \quad (14)$$

where  $jd \leq r \leq (j+1)d$ , and  $a = (1 - \phi_2)/\phi_2$ . The lineal-path function is trivially given by

$$L(r) = \begin{cases} \phi_2(1-r/d), & \text{when } 0 \leq r < d \\ 0, & \text{otherwise.} \end{cases} \quad (15)$$

The reference structure we adopt has a particle-phase volume fraction  $\phi_2$  equal to 0.5, and the length of the rods is chosen to be 10 pixels, giving a rod density of 50 per 1000 pixels. A realization of the reference structure and the  $S_2$ -reconstruction result are shown in Fig. 3. Note that while the  $S_2$  profile of the reconstructed system agrees strikingly well with that of the reference system, the visual images [Figs. 3(a) and 3(b)] do not appear to be similar. The rods in the reconstructed image clearly have a wide distribution of

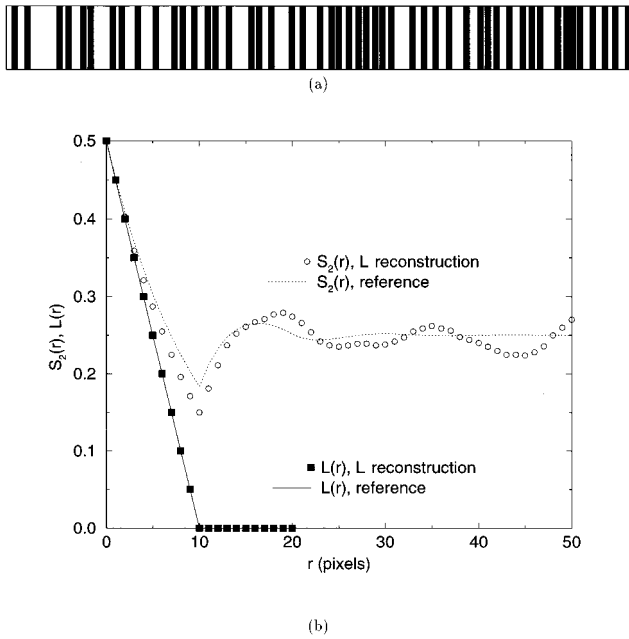


FIG. 4. (a)  $L$  reconstruction of equilibrium hard rods system. (b)  $L$  for the reference and reconstructed systems. Also shown is the two-point probability function  $S_2$  for both systems.

length, lacking the uniformity characteristics displayed in the reference system. A quantitative means of probing this non-uniqueness is to measure a *different* correlation function of the reconstructed system and compare it to the corresponding function of the reference system. Indeed, the lineal-path functions of the reference and reconstructed system (included in the figures) are seen to be significantly different for intermediate to large values of  $r$ . This example clearly shows that  $S_2$  does not generally contain sufficient information to uniquely determine a structure.

As stated earlier,  $L$  contains more clustering information than  $S_2$ , and it is therefore expected that  $L$  can capture the uniform nature of the rod length better. Indeed, this is the case, as shown in Fig. 4. Moreover, the  $S_2$  profile of the reconstructed image (measured *a posteriori*) is encouragingly close to that of the corresponding reference quantity. However, it is clear that the lineal-path function again does not ascertain a unique structure, i.e., any distribution of equisized rods (equilibrium of not) will give the same lineal-path function profile.

The hybrid ( $S_2 + L$ )-reconstruction result is shown in Fig. 5. The reconstructed structure is annealed to the extent that both correlation functions have little discrepancy from the reference ones. Visually, the structure seems to not differ substantially from that obtained by the  $L$  reconstruction, simply because the  $L$  reconstruction has already performed well in reconstructing the structure.

### C. Unphysical correlation functions

To push the reconstruction process ever further, we will investigate how the technique responds when a physically unrealizable reference correlation function is used. We notice from Eq. (7) or Eq. (8) that the slope of  $S_2(r)$  at  $r=0$  should

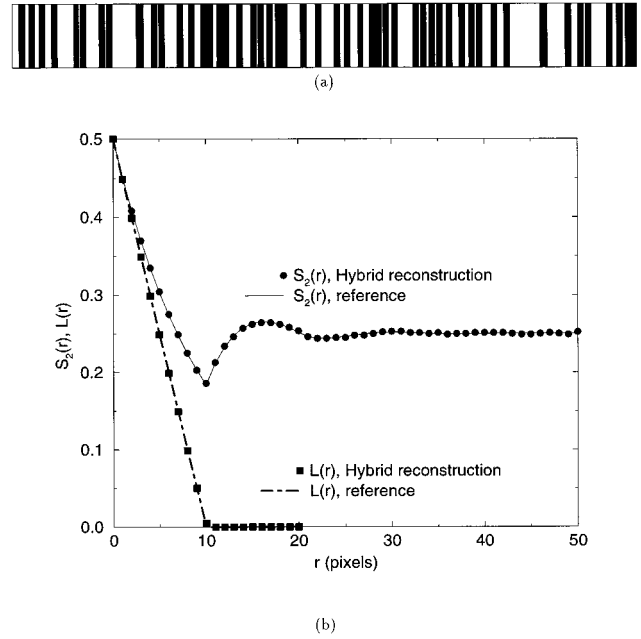


FIG. 5. (a) Hybrid reconstruction of equilibrium hard rods system. (b)  $S_2$  and  $L$  for the reference and reconstructed systems.

be negative for all physically realizable structures. One can therefore easily construct an unphysical reference  $S_2$  profile corresponding to a system with a *negative interfacial area* by assigning a positive slope at  $r=0$ . Such a reference function  $S_2$  and the corresponding reconstruction results are shown in Fig. 6. The reference  $S_2$  here has a positive slope at  $r=0$  and goes to its long-range value after 10 pixels.

It can be observed that the reconstruction procedure makes an effort to raise the slope of  $S_2$  at  $r=0$  as far as possible so as to approach the negative reference value.

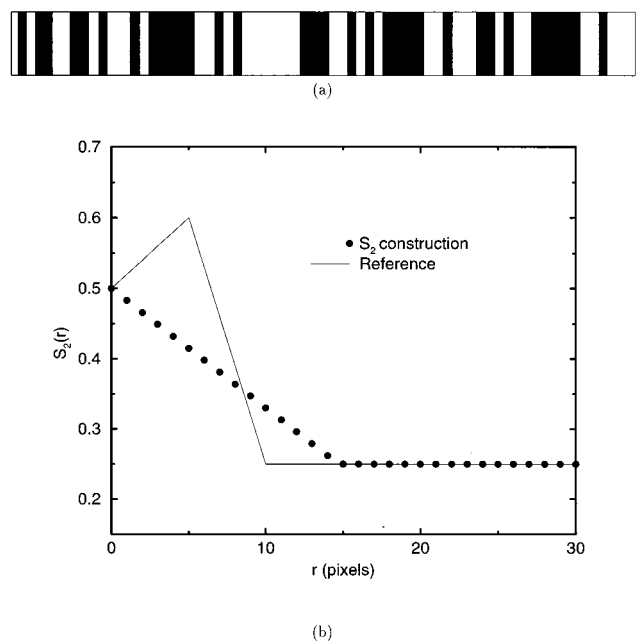


FIG. 6. (a)  $S_2$  construction of ‘negative interfacial area’ system. (b)  $S_2$  for the reference and constructed systems.

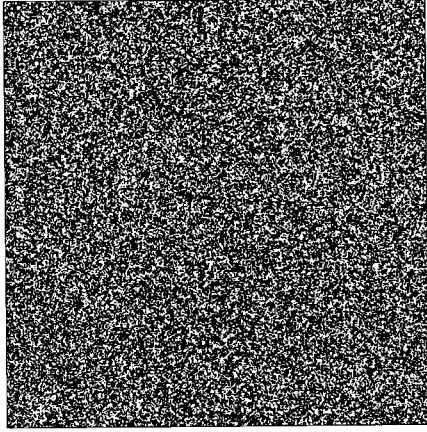


FIG. 7. Initial configuration: two-dimensional random checkerboard. System is  $400 \times 400$  pixels and volume fraction  $\phi_2 = 0.5$ .

However, the slope cannot increase too much since the resultant  $S_2$  profile is also constrained by the reference values at longer range to give minimum  $E$  in Eq. (1). Therefore, instead of annealing to a structure having a minimum  $s$  (which should contain only a single rod in the system), the reconstruction procedure gives a final structure consisting of

$$L(r) = \begin{cases} \frac{2\phi_2}{\pi} \left[ \cos^{-1}\left(\frac{r}{d}\right) - \frac{r}{d} \sin\left[\cos^{-1}\left(\frac{r}{d}\right)\right] \right], & \text{when } 0 \leq r < d \\ 0, & \text{otherwise.} \end{cases} \quad (16)$$

Clearly,  $L(r)$  is insensitive to the particular arrangement (e.g., equilibrium or RSA) of particles, provided that they are nonoverlapping equisized disks. The reference system is taken to have a particle-phase volume fraction  $\phi_2$  equal to 0.2. A realization of the reference system and the corresponding reconstruction results are shown in Fig. 8. Note that the  $S_2$  reconstruction again does not provide a satisfactory structure even though its  $S_2$  profile is in excellent agreement with the corresponding  $S_2$  of the reference system. The nonuniqueness issue arises again showing that the reconstructed system can match the original correlation function very well but yet has a significantly different structure. Similar to the 1D equilibrium rods case, the  $L$  reconstruction here gives a better result than  $S_2$  reconstruction in that the former better captures the size uniformity of the particles. That the particles are squarelike in shape is an artifact due to the evaluation of  $L$  in only two orthogonal directions. This defect could be eliminated by sampling in other directions, but of course, at the expense of computational cost. The hybrid ( $S_2 + L$ ) reconstruction, again similar to 1D case, gives only a slight improvement over the  $L$  reconstruction and hence this result is not shown here.

#### B. Random overlapping disks

The random overlapping disk model consists of spatially uncorrelated disks whose centers are determined by a Pois-

clusters of pixels such that  $s$  is the minimum under the constraint of the reference  $S_2$ .

#### IV. APPLICATION TO TWO-DIMENSIONAL MEDIA

In the 2D reconstruction, the initial system is taken to be a 2D random checkerboard of size  $400 \times 400$  pixels (unless otherwise stated), with the same volume fraction as the reference system. An example of a structure at 50% volume fraction is shown in Fig. 7. Again, phase 2 material will be the target of the reconstruction, which is represented by black pixels in the images.

##### A. Equilibrium hard disks

We begin by considering an equilibrium distribution of equisized hard disks of diameter  $d$  pixels. For disks with a diameter  $d$  greater than 15 pixels, the area of a digitized disk differs from that of the continuum disk by less than 1% [28]. We will take  $d > 15$  pixels to closely mimic the continuum result although the reconstruction procedure is not affected by the level of resolution.

The two-point probability function  $S_2$  of this system has been evaluated [26].  $S_2(i)$  ( $i =$  integer in terms of pixels) is obtained from a cubic-spline interpolation of the numerical data provided in Ref. [26]. The lineal-path function  $L$  for the particles can easily be derived analytically as

son process [29,23]. This is an interesting model in 3D because the system is bicontinuous (i.e., both phases are connected) when the particle volume fraction  $\phi_2$  lies in the interval  $[0.29, 0.97]$  [30,31]. In 2D, the system will never be bicontinuous, but it still captures nontrivial clustering information, and the particle-phase percolates at a volume fraction of about 68% [32]. The two-point probability function  $S_2$  of the system is given by [29]

$$S_2(r) = \exp[-\rho V_2(r)] + 1 - 2\phi_2, \quad (17)$$

where

$$V_2(r) = (\pi d^2)/2 - d^2/2 \{ \cos^{-1}(r/d) - (r/d) \sqrt{1 - (r/d)^2} \} H(d-r). \quad (18)$$

Here  $\rho$  is the number density of disks and  $H$  is the Heaviside step function. The lineal-path function is known analytically for the space exterior to the particles [18]. For the particle-phase,  $L$  is also known analytically but involves numerical evaluation [33]. We evaluate  $L$  instead by sampling over 1000 realizations of computer-generated digitized overlapping disks system.

It is of interest to examine the ability of the reconstruction algorithm to correctly reconstruct large clusters that may be

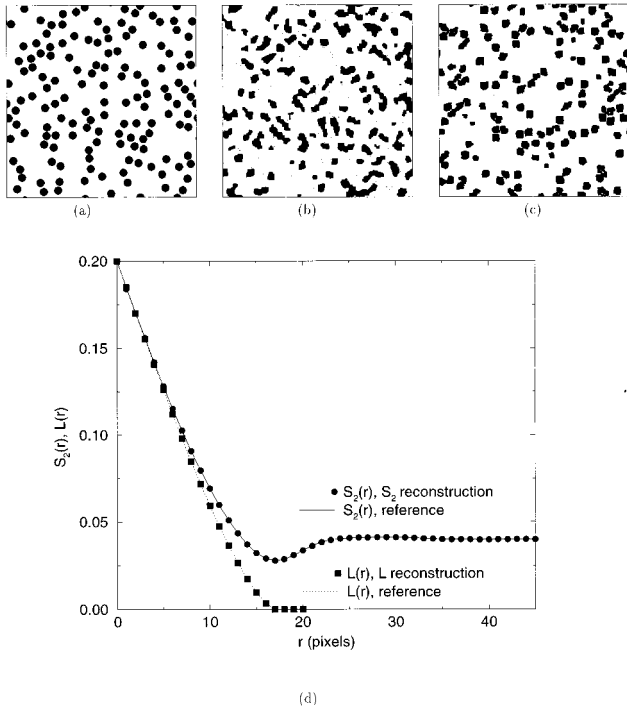


FIG. 8. (a) Reference system: a realization of equilibrium hard disks. System size =  $400 \times 400$  pixels, disk diameter = 17 pixels, and volume fraction  $\phi_2 = 0.2$ . (b)  $S_2$  reconstruction of equilibrium hard disks system. (c)  $L$  reconstruction of equilibrium hard disks system. (d)  $S_2$  for the reference and  $S_2$ -reconstructed systems, and  $L$  for the reference and  $L$ -reconstructed system.

present in a system. The reference system we used consists of disks with a diameter  $d = 31$  pixels. The size of the clusters is restricted by considering a particle-phase volume fraction  $\phi_2$  of 0.5, which is below the percolation threshold. A realization of the reference system and the reconstructions are shown in Fig. 9.

Not surprisingly, the  $S_2$  reconstruction does not give a good result: the cluster sizes are too large and the system actually percolates. We emphasize that the resulting  $S_2$  matches exactly the reference  $S_2$  profile (although the figure is not included here). The  $L$  reconstruction is superior to the  $S_2$  reconstruction, capturing the cluster distributions better. However, the hybrid ( $S_2 + L$ ) reconstruction apparently outperforms the previous two methods. The resultant correlation function profiles are compared to the corresponding reference profiles in Fig. 10. It should be mentioned that the requirements for this reconstruction are demanding in that 50% of the pixels in a very large system ( $400 \times 400$  pixels) are required to aggregate in such a way as to form large clusters that have reasonable shape. It can be seen that the hybrid reconstruction successfully accomplishes this task. This example clearly shows that combinations of correlation functions in the reconstruction procedure can yield a much better result than those using single ones.

### C. Debye random media

Debye claimed without rigorous proof that the exponentially decay two-point probability function given by

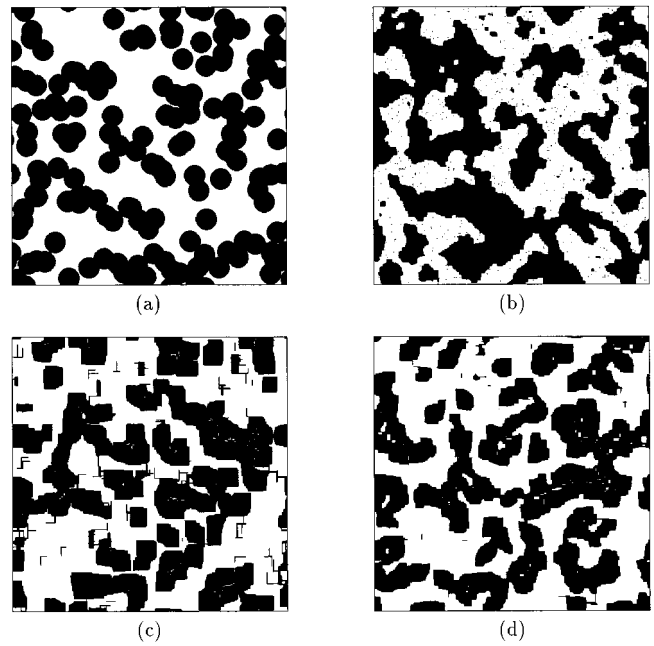


FIG. 9. (a) Reference system: a realization of random overlapping disks. System size =  $400 \times 400$  pixels, disk diameter = 31 pixels, and volume fraction  $\phi_2 = 0.5$ . (b)  $S_2$  reconstruction of random overlapping disks system. (c)  $L$  reconstruction of random overlapping disks system. (d) Hybrid reconstruction of random overlapping disks system.

$$\frac{S_2(r) - \phi_2^2}{\phi_1 \phi_2} = \exp(-r/a), \quad (19)$$

where  $a$  is a correlation length, applies to structures in which one phase consists of “random shapes and sizes” [24,25]. It is now known that certain types of space tessellations have two-point functions given by Eq. (19) [34,35]. We refer to this class of structures as *Debye random media*.

We are also in a position to find the specific structures that realize the function given by Eq. (19). We chose  $\phi_2$

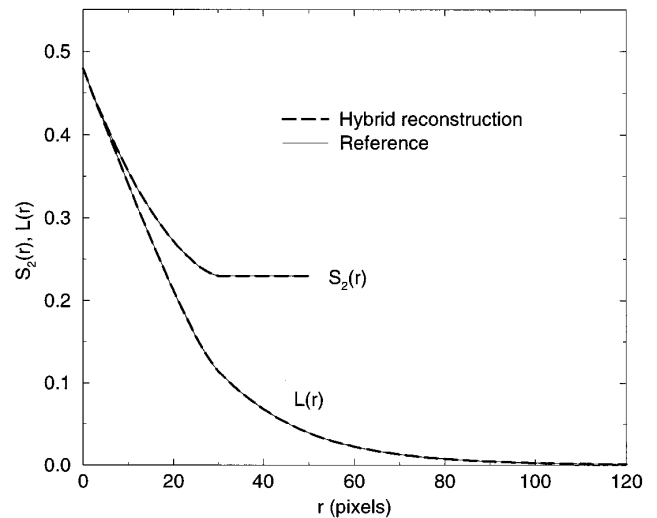


FIG. 10.  $S_2$  and  $L$  for the reference and hybrid reconstructions of the random overlapping disk system.

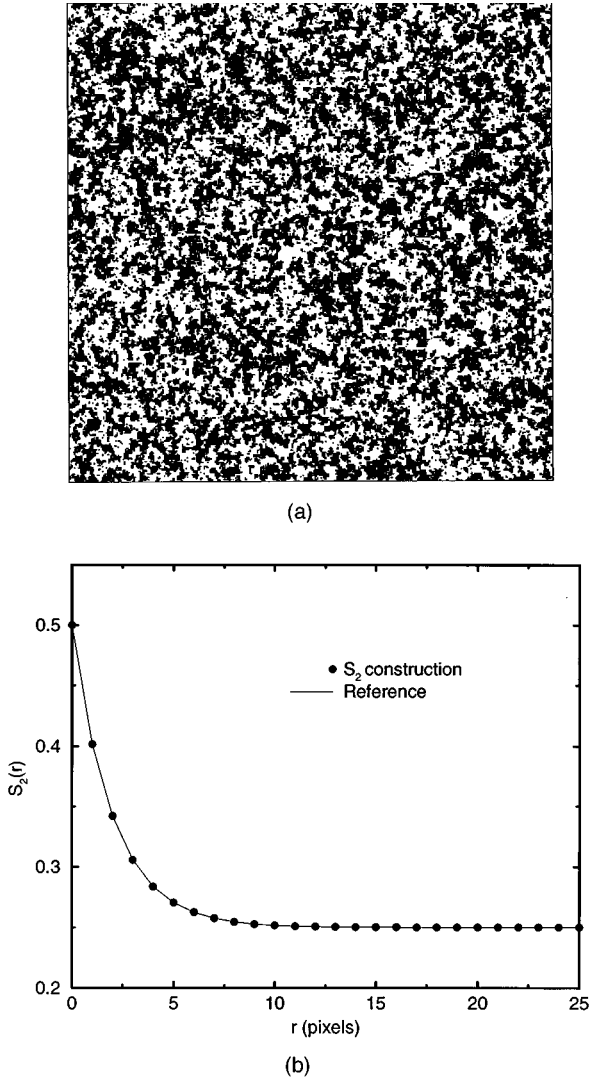


FIG. 11. (a)  $S_2$  construction of a “Debye random medium.” System size =  $400 \times 400$  pixels, volume fraction  $\phi_2 = 0.5$ , and correlation length  $a = 2$  pixels. (b)  $S_2$  for the reference and constructed system.

$= 0.5$  and  $a = 2$  pixels for the construction procedure. The construction results are shown in Fig. 11. The resulting structure is seen to be consistent with Debye’s intuitive description of it. This successful example serves as a prelude to the generation of hitherto unknown structures from specified correlation functions.

#### D. Hypothetical medium

We will now illustrate one of the powerful aspects of the reconstruction procedure, namely, the ability to generate heretofore unknown structures from hypothetical correlation functions. In this section, we will use a physically realizable correlation function, but in the next section, we will employ physically unrealizable ones. Here we will assume that the two-point probability function is given by the exponentially damped, oscillating function

$$\frac{S_2(r) - \phi_2^2}{\phi_1 \phi_2} = \exp(-r/a) \cos(\omega r + \psi), \quad (20)$$

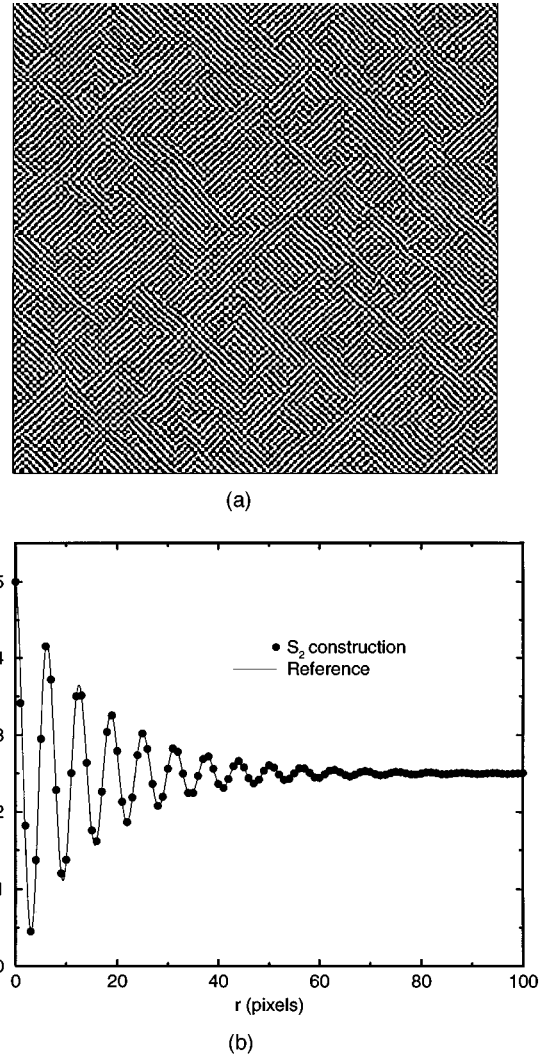


FIG. 12. (a)  $S_2$ -construction for a system with an exponentially damped, oscillating correlation function specified by Eq. (20). System size =  $400 \times 400$  pixels, volume fraction  $\phi_2 = 0.5$ , correlation length  $a = 8$  pixels,  $\omega = 1$  (pixel) $^{-1}$ , and phase angle  $\psi = 0$ . (b)  $S_2$  for the reference and constructed system.

where the parameter  $a$  bounds the amplitude of the  $S_2$  profile,  $\omega$  is the wave number, and  $\psi$  is the phase angle. It is immediately obvious that the corresponding medium should have two different characteristic length scales. One of the length scales is dictated by the wave number  $\omega$  and the other one by  $a$ , which is the correlation length of the bulk features of the medium. We adopt  $a = 8$ ,  $\omega = 1$ , and  $\psi = 0$  in the construction. The reference correlation function profile is shown in Fig. 12.

The generated structure corresponding to Eq. (20) [see Fig. 12(a)] has a labyrinthine appearance. As expected from the form of the reference correlation function, this structure is highly correlated and the two different characteristic length scales can clearly be identified. The shorter characteristic length scale is the average width of the “wall” of the labyrinth (shown as black pixels in the figure), which is of the order of  $\pi/\omega$ . The value of  $S_2$  at this distance is the minimum of the  $S_2$  profile, indicating that the correlation immediately beyond this distance is negligible (see also the

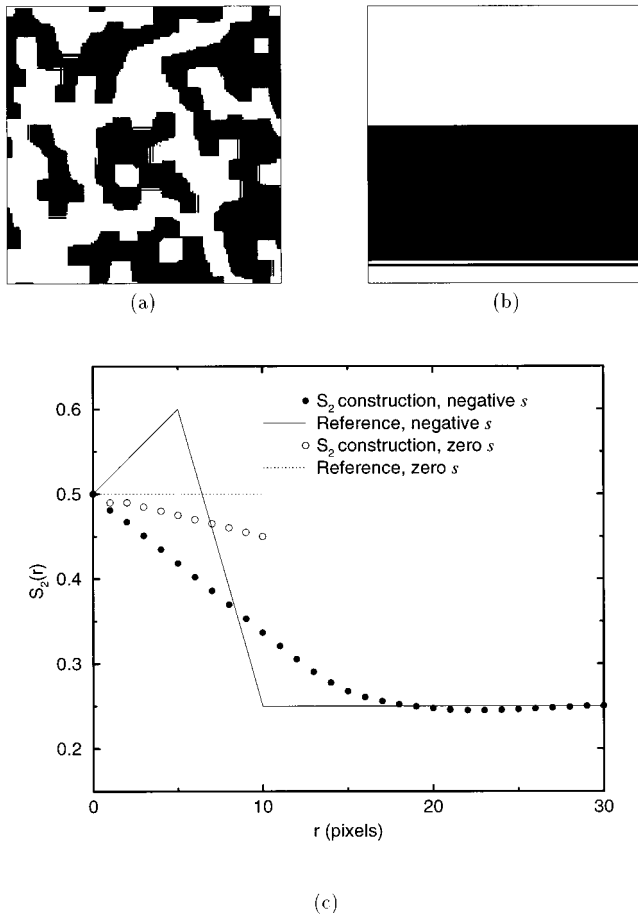


FIG. 13. (a)  $S_2$  construction of “negative interfacial area” system. System size =  $200 \times 200$  pixels and volume fraction  $\phi_2 = 0.5$ . (b)  $S_2$  construction of “zero interfacial area” system. System size =  $100 \times 100$  pixels and volume fraction  $\phi_2 = 0.5$ . (c)  $S_2$  for the reference and constructed systems.

$S_2$  profiles of equilibrium hard rods and disks). On the other hand, the average size of the “patches” (where the labyrinth walls orient in the same direction) is governed by the correlation length  $a$ .

This example serves to illustrate that the reconstruction algorithm is capable of generating structures that match hypothetical, physically realizable correlation functions that are rather complicated functionally. Moreover, by examining the generated structures, we will be able to deepen our understanding of the nature of the information contained in these correlation functions.

### E. Unphysical correlation functions

We now tax the procedure in two dimensions by employing unphysical correlation functions, as we did in one dimension. The same reference  $S_2$  that gave physically unrealizable 1D structures with negative  $s$  is used here [see Fig. 13(c)], but with a system size of  $200 \times 200$  pixels. The resultant structure shown in Fig. 13(a) consists of large clusters in order to minimize  $s$  as much as physically possible. Similar to the 1D case, this annealed structure is not comprised of a single cluster that has the minimum  $s$ . Again, this is because the structure is constrained by the reference  $S_2$  after

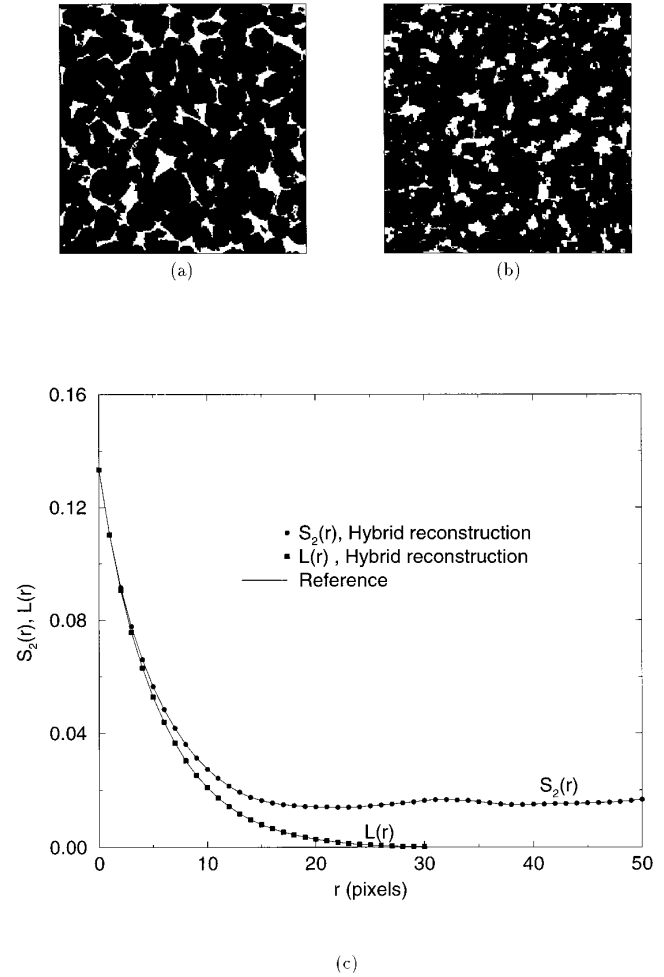


FIG. 14. (a) Reference system: a section of Fontainebleau sandstone. System size =  $280 \times 280$  pixels. White pixels are void phase, and black pixels are material phase. (b) Hybrid reconstruction of Fontainebleau sandstone. (c)  $S_2$  and  $L$  for the reference and hybrid reconstruction systems.

$r=0$ , which the algorithm tries to match as closely as possible while yielding a realistic structure.

Another unphysical example that we study has a constant  $S_2$  at a value of  $\phi_2$  for any  $r$  [see Fig. 13(c)]. This implies that the reference structure has to have a zero specific surface area. Unlike the previous case, the fact that the reference  $S_2$  always remains at the highest value ( $\phi_2$ ) means that there is no constraint by the reference  $S_2$  to restrict the largest slope a physical structure can achieve [i.e., higher slope will favorably yield lower  $E$  in Eq. (1) at the same time]. The value of  $\phi_2$  that we used here is 0.5 and the system size is  $100 \times 100$  pixels. The generated structure shown in Fig. 13(b) indeed indicates that the nearest feasible structure such correlation function can have is a structure consisting of one large percolating cluster, which has the minimum specific surface area possible.

### F. Fontainebleau sandstone

Having obtained reasonably successful reconstruction results for theoretical model systems, we are in a position to explore the reconstruction of real random media. We will

reconstruct a tomographic image of a slice of Fontainebleau sandstone as obtained from the study of Coker, Torquato, and Dunsmuir [36]. The image is shown in Fig. 14(a). The size of the filtered image extracted is  $280 \times 280$  pixels, where one pixel equals  $7.5 \mu\text{m}$ . In this case, for efficiency purposes, the target phase to be reconstructed is the disconnected void phase, represented as white pixels in the image. The reference correlation functions of the true sandstone are obtained by the sampling techniques described in Secs. II B and II C, respectively, but modified to accommodate the non-periodic boundary conditions of the image.

We found that both the single  $S_2$  reconstruction and the single  $L$  reconstruction did not capture the salient structural features of the sandstone as satisfactorily as the hybrid reconstruction and hence we just report the latter result. The overall features of the hybrid reconstructed image [shown in Fig. 14(b)] closely resembles the original sandstone image, except that the void regions are typically more rounded in shape. Note that the  $S_2$  and  $L$  profiles of the reconstructed medium match well the corresponding profiles of the true sandstone [see Fig. 14(c)]. Naturally, the minor differences between the images should diminish if more correlation functions are employed and sampling is performed in more directions.

## V. CONCLUSIONS

In this paper, we have presented a simple yet powerful procedure to reconstruct digitized random media from limited morphological information. The procedure is capable of reconstructing multidimensional, multiphase, and anisotropic structures. We applied the methodology to reconstruct a number of 1D and 2D model microstructures as well as a real sandstone image using the morphological information contained in the two-point correlation function  $S_2$  alone, the lineal-path function  $L$  alone, and both  $S_2$  and  $L$ . For the 1D periodic models, the reconstructions were perfect. For the random cases, the reconstructions generally captured the sa-

lient features of the reference systems. However, even though the reference and reconstructed correlation functions matched well, the reconstructions deviated somewhat from the reference systems as measured by differences in other correlation functions of the system. This nonuniqueness is expected since lower-order correlation functions generally do not contain complete morphological information. It will be of interest to test the sensitivity of the macroscopic properties of the systems.

We also used our algorithm to address another intriguing inverse problem, namely, the construction of heterogeneous media based on the specification of model or hypothetical statistical correlation functions [1], including physically unrealizable correlation functions. This question involves understanding the general mathematical properties of realizable correlation functions, which thus far has not been fully explored. Moreover, there are a family of structures that can have the same correlation function and there may be many structures within this family that possess similar effective properties. However, as noted by Torquato [1], it is likely that some structures within this family will have markedly different effective properties and it would be of interest to identify the *outliers*. Understanding this question of nonuniqueness as it relates to the effective properties of heterogeneous media will offer great insight into structure/property relations.

We are extending the procedure to reconstruct 3D isotropic structures from 2D slices of the material and to more complex media, such as anisotropic structures. We will also compare the macroscopic properties of the reference systems to the corresponding properties of the reconstructed systems. Such work will be reported in future publications.

## ACKNOWLEDGMENT

We gratefully acknowledge the support from the U.S. Department of Energy, Office of Basic Energy Sciences under Grant No. DE-FG02-92ER14275.

- 
- [1] S. Torquato, *Int. J. Solids Struct.* (to be published).
  - [2] M. Joshi, Ph.D. thesis, University of Kansas, Lawrence, 1974.
  - [3] J. A. Quiblier, *J. Colloid Interface Sci.* **98**, 84 (1984).
  - [4] P. M. Adler, C. G. Jacquin, and J. A. Quiblier, *Int. J. Multiphase Flow* **16**, 691 (1990); P. M. Adler, C. G. Jacquin, and J. F. Thovert, *Water Resour. Res.* **28**, 1571 (1992).
  - [5] P. M. Adler, *Porous Media: Geometry and Transport* (Butterworth-Heinemann, Boston, 1992).
  - [6] J. Poutet, D. Manzoni, F. Hage-Chehade, C. G. Jacquin, M. J. Boutéca, J. F. Thovert, and P. M. Adler, *Int. J. Rock Mech. Min. Sci. Geomech. Abstr.* **33**, 409 (1996).
  - [7] M. Giona and A. Adrover, *AIChE. J.* **42**, 1407 (1996).
  - [8] J. W. Cahn, *J. Chem. Phys.* **42**, 93 (1965).
  - [9] N. F. Berk, *Phys. Rev. Lett.* **58**, 2718 (1987).
  - [10] N. F. Berk, *Phys. Rev. A* **44**, 5069 (1991).
  - [11] M. Teubner, *Europhys. Lett.* **14**, 403 (1991).
  - [12] A. P. Roberts and M. Teubner, *Phys. Rev. E* **51**, 4141 (1995).
  - [13] A. P. Roberts and M. A. Knackstedt, *Phys. Rev. E* **54**, 2313 (1996).
  - [14] P. Levitz (unpublished).
  - [15] M. D. Rintoul and S. Torquato, *J. Colloid Interface Sci.* **186**, 467 (1997).
  - [16] M. P. Allen and D. J. Tildesley, *Computer Simulation of Liquids* (Clarendon Press, Oxford, 1987).
  - [17] S. Torquato and G. Stell, *J. Chem. Phys.* **77**, 2071 (1982).
  - [18] B. Lu and S. Torquato, *Phys. Rev. A* **45**, 922 (1992).
  - [19] S. Torquato, J. D. Beasley, and Y. C. Chiew, *J. Chem. Phys.* **88**, 6540 (1988).
  - [20] S. Torquato and B. Lu, *Phys. Rev. E* **47**, 2950 (1993).
  - [21] A. E. Scheidegger, *The Physics of Flow Through Porous Media* (University of Toronto, Toronto, Canada, 1974).

- [22] S. Torquato and M. Avellaneda, *J. Chem. Phys.* **95**, 6477 (1991).
- [23] See the review of S. Torquato, *Appl. Mech. Rev.* **44**, 37 (1991), and references therein.
- [24] P. Debye and M. Bueche, *J. Appl. Phys.* **20**, 518 (1949).
- [25] P. Debye, H. R. Anderson, Jr., and H. Brumberger, *J. Appl. Phys.* **28**, 679 (1957).
- [26] S. Torquato and F. Lado, *J. Phys. A* **18**, 141 (1985).
- [27] J. Quintanilla and S. Torquato, *Phys. Rev. E* **53**, 4368 (1996).
- [28] E. J. Garboczi, M. F. Thorpe, M. DeVries, and A. R. Day, *Phys. Rev. A* **43**, 6473 (1991).
- [29] H. L. Weissberg, *J. Appl. Phys.* **34**, 2636 (1963).
- [30] M. D. Rintoul and S. Torquato, *J. Phys. A* **30**, L585 (1997).
- [31] J. Kertész, *J. Phys. (Paris) Lett.* **42**, L393 (1981).
- [32] M. Rosso, *J. Phys. A* **22**, L131 (1989).
- [33] J. Quintanilla and S. Torquato, *Phys. Rev. E* **54**, 4027 (1996).
- [34] D. Stoyan, W. S. Kendall, and J. Mecke, *Stochastic Geometry and its Applications* (John Wiley & Sons, New York, 1987).
- [35] V. K. Oganian, *Dokl. Akad. Nauk. Armenian SSR* **58**, 193 (1973).
- [36] D. A. Coker, S. Torquato, and J. H. Dunsmuir, *J. Geophys. Res.* **101**, 17 497 (1996).